Joint analysis of the Super-Sauze (French Alps) mudslide by nanoseismic monitoring and UAV-based remote sensing

Marco Walter,[1*] Uwe Niethammer,[1] Sabrina Rothmund[1] and Manfred Joswig[1] **report on how the study of landslide dynamics at locations like the Super-Sauze mudslide in the French Alps have benefited from emerging methods such as nanoseismic monitoring and unmanned aerial vehicle remote sensing by resolving surface fractures and mudslide-bedrock interaction.**

Due to global climate change and the fact that mountain areas will become inhabited at a progressive rate, landslides pose a huge threat to the environment, the infrastructure and the people living in the vicinity of affected areas. In inhabited regions landslides can cause enormous economic damage and unfortunately human losses as well. Slope instabilities are caused by the non-linear interaction of geological, hydrological, morphological, and soil mechanical processes on many scales in time and space. Models for the prediction of landslides are very vulnerable because the influencing parameters are still incompletely or unsatisfactorily observed. Therefore the observation of landslides by multiple disciplines is the challenge of recent studies. Integrated analysis should reveal further insights into the process interactions and the complex behaviour of landslides.

Our research is highly motivated by newly improved measuring techniques that can resolve specific landslide parameters at higher resolution, and in repeat observations. We can determine landslide dynamics using nanoseismic monitoring (Joswig, 2008) and UAV-based (unmanned aerial vehicle) high-resolution remote sensing (Niethammer et al., 2009). With the former, one can resolve fracture processes in the shallow subsurface (Walter and Joswig, 2008; Walter and Joswig, 2009). The latter technique is especially suited for mapping the corresponding photo-lineaments at the slope's surface. Our geophysical investigations were carried out at the Super-Sauze, French Alps mudslide (Figure 1) and the Heumoes, Austrian Alps slope. They are part of the research project 'Coupling of flow and deformation processes for modelling the movement of natural slopes' (www.grosshang.de).

Applying geophysical methods like active seismics, ground penetrating radar, and geoelectrical mapping and sounding, Grandjean et al. (2007) inferred dynamic processes and static properties for the mudslide in Super-Sauze. Single fracture processes during the movement of landslides consisting of hard rock (fragments) have been seismically monitored in the Alps (e.g., Brückl and Mertl, 2006; Spillmann et al., 2007) and in Norway (Roth et al., 2005). Fracturing within creeping landslides consisting of weak sediments radiates signals of much smaller energy; it has first been observed, to our knowledge, by Walter and Joswig (2008) applying the nanoseismic monitoring method.

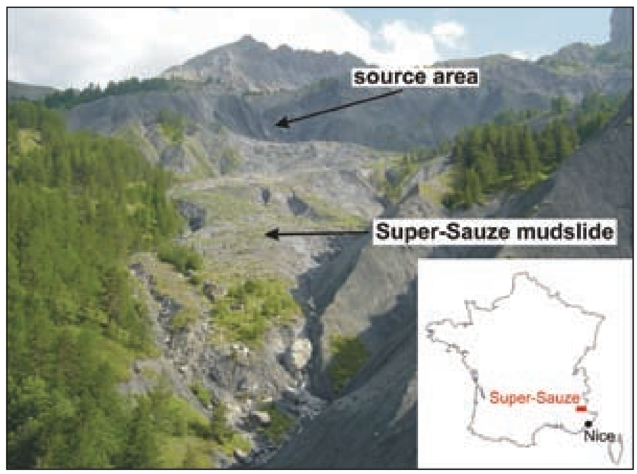

Figure 1 Location of Super-Sauze and upward view of the mudslide and its source area. Picture was taken in summer of 2006.

Here we describe how the seismic monitoring of the slope's subsurface is combined with the UAV-based remote sensing of the surface. By remotely sensing the active slope, its dimensions and surface structures can be characterized (Niethammer et al., 2009). Aerial images taken by satellites or airplanes have spatial resolutions of metres to decimetres. They can be used for landslide detection and to determine deformations on a large scale (Henry et al., 2002). UAV-based remote sensing is suited to map surface structures with high spatio-temporal resolution, e.g., fissure patterns on landslides with centimetre resolution and monthly overflight. In particular, it is possible to detect and analyze dislocation vectors on landslides from these data (Niethammer et al., 2009).

[1] *Institute for Geophysics, Universität Stuttgart, Azenbergstraße 16, 70174 Stuttgart, Germany.*
* *Corresponding author, E-mail: Marco.Walter@geophys.uni-stuttgart.de*

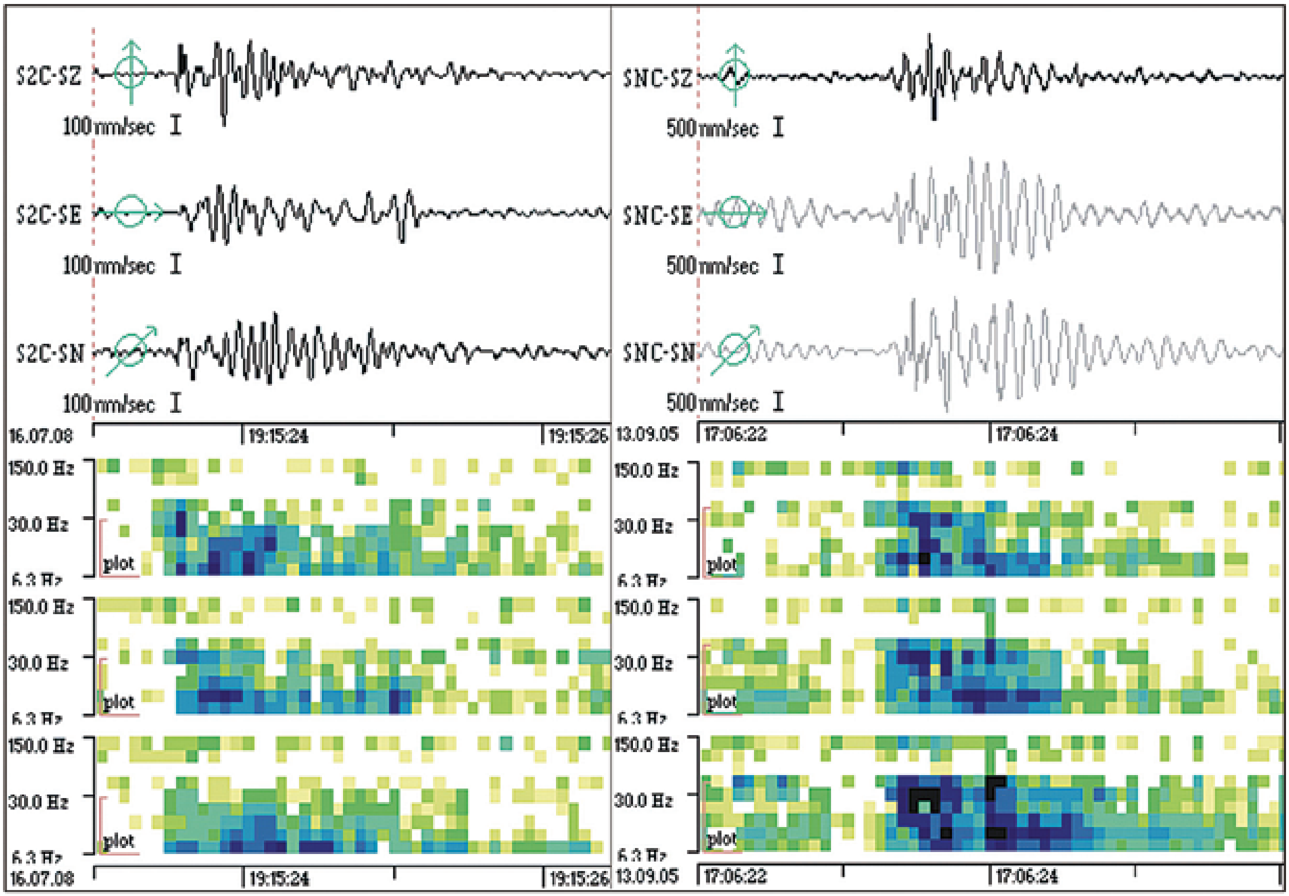

Figure 2 Typical seismograms and sonograms of deformation processes caused by softrock-landslides, recorded with a 3c-seismometer: Left: 'fracture' event, M_L = -2.2 in ~120 m distance, recorded at the Super-Sauze mudslide Right: fracture process of M_L = -1.2 in ~100 m distance observed at the Heumoes slope. Modified after Walter and Joswig 2008, 2009.

Observation of slope dynamics by nanoseismic monitoring

Nanoseismic monitoring acts as a seismic 'microscope' to detect small impulsive signals in the subsurface, and was first applied to map sinkholes in Israel (Wust-Bloch and Joswig, 2006). We used the method to monitor fracture processes at the Heumoes slope, Austria (Walter and Joswig, 2008). Like the Super-Sauze mudslide, the Heumoes slope consists of weak sediments. The existence of impulsive seismic signals wasn't expected due to the presumed lack of brittle material that could generate impulse fracture release. The increased sensitivity available from nanoseismic monitoring was needed to discover these local fracture processes in sediments at all.

Data acquisition/data processing

In Super-Sauze, the seismic data was acquired during a 10-day field campaign in July 2008 deploying four tripartite seismic mini arrays on the mudslide (Figure 4). Each mini array, so-called seismic navigating system (SNS) consists of one three-component and three vertical, short-period seismometers installed with an aperture of 30–40 m. Data was recorded in continuous mode with a sampling rate of 400 Hz. The observation period was limited to 10 days because nanoseismic monitoring resembles more a campaign of refraction seismics, than a permanent seismic network installation. It achieves its superior sensitivity by not compromising in site selection (e.g., demands for shelter, power, communications) or on cost of increased vulnerability by extended array cabling. The data set was processed using the software HypoLine, an interactive, graphical jack knife tool which displays the most plausible solution for low-SNR (signal to noise ratio) signals, resolving the influence of individual parameters on the event localization in real-time (Joswig, 2008).

Signal classification

From seismic data analysis, we could detect different types of events caused by the dynamics in the source area of the mudslide, and within the slope itself. The signals vary in duration, amplitude, frequency content, and consequently in sonogram patterns (Walter and Joswig, 2009). We could distinguish three principal types of events: The 'rockfall' events occur in the source area of the mudslide while the events of type 'fracture' and type 'scratch' are caused within the mudslide body during its deformation. The classification of the observed signals is described in detail by Walter and Joswig (2009). For the joint analysis of the mudslide dynamics in Super-Sauze by nanoseismic monitoring and UAV-based remote sensing, we focus on the characteristics and locations of the 'fracture' and 'scratch' events.

Seismic signals caused by failure of the slope material

We could detect 34 'fractures', which show clear phase onsets (Figure 2), allowing for their localization by standard seismological procedures. The duration of these events lies between 2–5 seconds, the maximum amplitude varies between 40 and 200 nm/s (peak to peak) and the frequency content is concentrated between 10–80 Hz. The signals had to be recorded on at least 2 SNS for being localized, where the distance range for reliable detection was within some 200 m. The emergent onset, the lack of higher frequencies above 80 Hz, and the signal incoherency indicate intense scattering caused by the high heterogeneity of slope material (Figure 2). Comparable signals have been observed on the Heumoes slope, which consists of soft rock material as well (Walter and Joswig, 2008). The magnitudes of 'fractures' at Super-Sauze vary between $-3.2 \leq M_L \leq -1.3$. This range is about one magnitude lower than at Heumoes slope ($-2.2 \leq M_L \leq -0.7$) indicating a 10 times lower ambient noise level in Super-Sauze.

The localized fractures are mainly clustered in the middle part of the mudslide (Figure 4). The cluster correlates with the part of the slope showing the highest velocities at the surface. The three events located in the south, outside of the slope catchment, are probably generated by material failure in the hard rock mass in the source area of the mudslide (Figure 4). Another cluster of 'fractures' is located directly at the boundary between the mudslide material and one of the emerging in-situ crests in the middle part of the slope. The estimated detection threshold for these events is $M_L = -2.6$ for a slant distance of about 140 m. The estimated localization accuracy is about 10 % of the epicentral distance. As the source depth could not be determined due to the sparse station distribution, it is not possible to estimate at which depth nor along which material interface the source processes took place.

Furthermore, we recorded 44 signals showing significant differences compared to the 'fracture' impulses. They occur as sequences lie barely above the ambient noise level and could not be observed at Heumoes slope due to the tenfold higher noise level there. These 'scratch' events haven't been expected previously. Their duration varies between 2–20 seconds, and the small amplitudes were only recorded at one single SNS. Compared to 'fractures', signal energy is prevailing at higher frequencies up to 150 Hz (Figure 3). Enormous attenuation effects can be seen within one single SNS with decay of signal amplitude by a factor of thirty. No distinct phase onsets could be identified, thus we just estimated the source area close to the station with highest amplitude. Figure 4 shows the quantity of these 'scratch' events at each station. Like the 'fracture' locations, most of the 'scratch' events occurred in the middle part of the slope. The source area of 64 % of these events is estimated to be close to the station S2E, at the boundary of the slope material and one of the emerging in-situ crests.

UAV-based remote sensing of the mudslide

The Super-Sauze mudslide was imaged in October 2008 using a self-designed quad-rotor remote sensing platform. The achievable flight height over ground is 20 m to 200 m, resulting in ground resolutions between 1–8 cm per pixel. This high resolution is essential to detect small fissure patterns at the surface. Quad-rotor systems basically enable close-range photographs of any desired area. Compared to conventional helicopters, quad-rotor systems do not require mechanical steering of the rotors and are stabilized by inertial measurement sensors (IMU). Especially in alpine terrain, like at the mudslide in Super-Sauze, such robust and reliable UAV-systems have considerable advantages. Open source projects are available to provide quad-rotor software and hardware (UAVP, 2008; Mikrocopter, 2008). The quad-rotor system and its main features are illustrated in Figure 5.

Image acquisition/image processing

The installed compact camera suffers from optical distortion in the wide-angle range (barrel distortion). In a first processing step this distortion of all acquired photographs was corrected by a polynomial correction approach. In a second step, plane

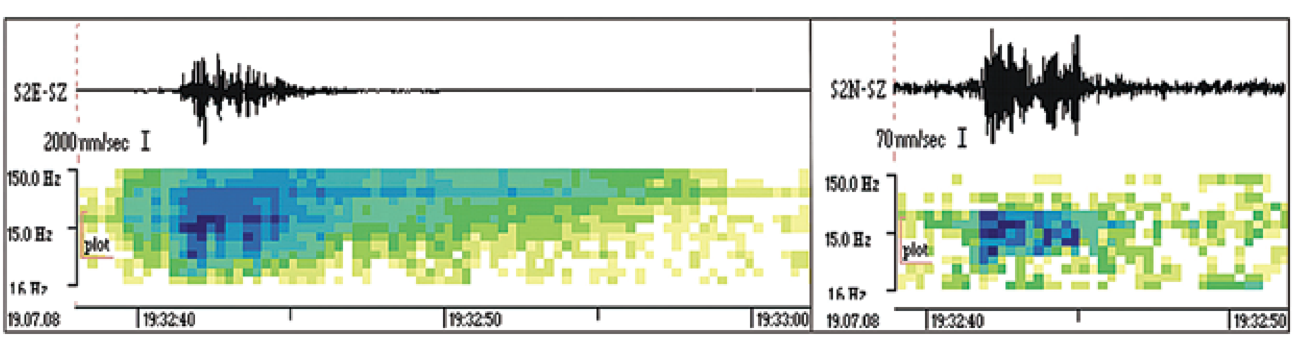

***Figure 3** Typical waveforms and sonogram patterns of one 'scratch' sequence, recorded with a 1c-station close to the source location (left) and with a 1c-station in a distance of ~25m (right). Modified after Walter and Joswig 2009.*

image rectification was applied to all images. The necessary ground information was gained by 199 ground control points (GCP) on the surface of the mudslide, measured by a differential GPS system with an accuracy of a few cm. This information was also necessary for the further geocoding of the pictures. In a third step, 59 rectified photographs were combined to one high resolution ortho-mosaic. Errors could be identified by comparison of the visible GCP locations in the photograph to the DGPS-measured locations, using a geographic information system (GIS). Areas which still showed ineligible errors in rectification were cut out manually before the final assembly of the rectified images was performed. The uniformly coloured mosaic was gained by colour balance correction in conjunction with an image-blending algorithm.

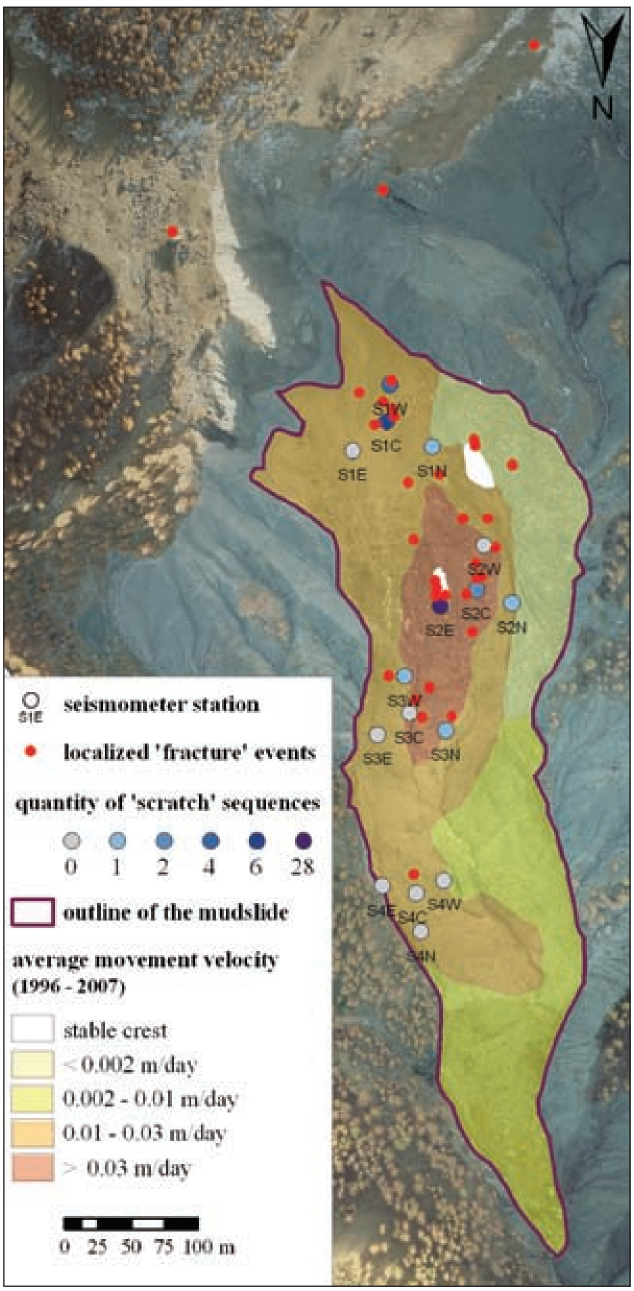

Figure 4 Location of the installed seismometer stations (circles), epicentres of the located 'fractures' (red) and the quantity of 'scratch' sequences recorded at each station (blue colour scale). Underlayn is the map of the average movement velocities of the mudslide (1996-2007).

Displacement analysis

In May 2007 an aerial LIDAR scan of the Super-Sauze mudslide was acquired, and on this basis another DTM and ortho-photograph were created. The spatial resolution of the DTM data is 1.0 m, the resolution of the ortho-photograph is about 0.25 m. The image analysis was carried out by the comparison of the geocoded ortho-photograph from 2007 and the geocoded ortho-mosaic of our UAV-based campaign in October 2008 (Niethammer et al., 2009).

Superficial displacement rates were identified directly, comparing the locations of rocks, stones, and parts of vegetation patches between the ortho-photograph from 2007 and our acquired ortho-mosaic from 2008. These measurements were performed manually within a GIS. Hence, between May 2007 and October 2008, displacements of 7.1 m–55.4 m were detected. The maximum deviation reaches 3.9 m, the mean error can be quantified to be 0.5 m.

However, areas which were characterized by extremely high displacement rates couldn't be compared, since no clear detectable features were left on the surface. In some areas it is likely that fine-grained sediments originating from debris flows cover the main features. The crown of the slope, the source area, is characterized by enormous dynamics, e.g., rockfalls, which cover these structures as well.

The identified displacement vectors were converted to daily displacement rates and compared to long-term displacement measurements between 1996–2007, acquired by laser scanning and DGPS measurements (Amitrano et al., 2007, Figure 6).

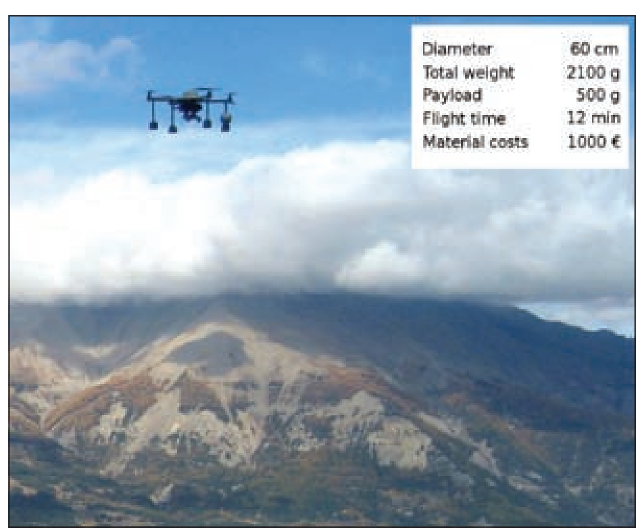

Figure 5 Quad-rotor system for remote sensing and its main characteristics. Here in use at the mudslide in Super-Sauze.

The displacement rates of our studies are up to ten times higher in the source area, and in the remaining part of the landslide approximately two times higher than the average movement rates. This deviation might be explained by higher dynamics in recent years, but the location of the strongest dynamics did not change.

Analysis of fissure patterns

The spatial resolution of the acquired UAV-based ortho-mosaic allows for detailed analysis of fissure structures. The hard rock boundaries of the Super-Sauze mudslide are very complex caused by the diversified former topography, comparable to badlands, consisting of buried crests and gullies. As the dynamics of the mudslide are high, the behaviour of the slope can be compared to glaciers, with similar fissure structures observed at the surface. Fissure structures on glaciers have been thoroughly investigated (Hambrey and Alean, 1994; Hambrey and Lawson, 2000; Wilhelm, 1975). In our context, fissure patterns on glaciers can be compared to the ones we observed at Super-Sauze. From their spatio-temporal occurrences one can learn about their development, and consequently about the behaviour of the entire mudslide.

As shown in Figure 7, there are several structures at the mudslide's surface which differ in shape and orientation. The structures could be identified as longitudinal fissures, transversal fissures, shear fissures, and cross-shaped fissures. The occurrence of those tension cracks depend on the bedrock topography, as well as on the lateral hard rock boundary, cavity, and extension in the longitudinal direction of movement, and changes in the decline of the slope (Wilhelm, 1975). Longitudinal fissures mostly occur after a cavity in the longitudinal direction of the movement, where an increased extension is initiated (Hambrey and Alean, 1994); such structures are shown in Figure 7d. The cavity of the stream can be explained by a curved crest in this area hidden by the mudslide material today (Figure 8). Transversal fissures often can be observed in areas where changes in the decline of the slope are present (Varnes, 1978; Hambrey and Alean, 1994; Wilhelm, 1975); comparable structures on the mudslide are shown in Figure 7c. In this particular case, the change of the decline of the slope can be explained by the secondary scarp in this area.

Marginal or shear fissures mostly occur at the boundary area between solid rock margins and the landslide material, resulting in a velocity transition (Wilhelm, 1975). These fissures run in accordance with the shear-strain conditions and start from the solid rock boundary with an angle of 30°–45° up the slope in the direction of the sliding body (Wilhelm, 1975; Hambrey and Alean, 1994, Figure 7a). Beside these patterns we observed 'cross-shaped' fissures, which are probably caused by an unknown combination of these dynamics (Figure 7b). Despite an apparent movement of the sliding surface, fissures linger on the same place. These cross-shaped fissures are obviously a result of tension changes caused by the change of the bedrock-topography in form of in-situ crests within the mudslide material (Figure 8).

Joint interpretation

The observation of mudslide subsurface dynamics by nanoseismic monitoring and the mapping of fissure patterns at surface by UAV-based remote sensing can be combined in a joint interpretation that compensates for inherent weaknesses of each method. In the given field lay out, nanoseismic monitoring

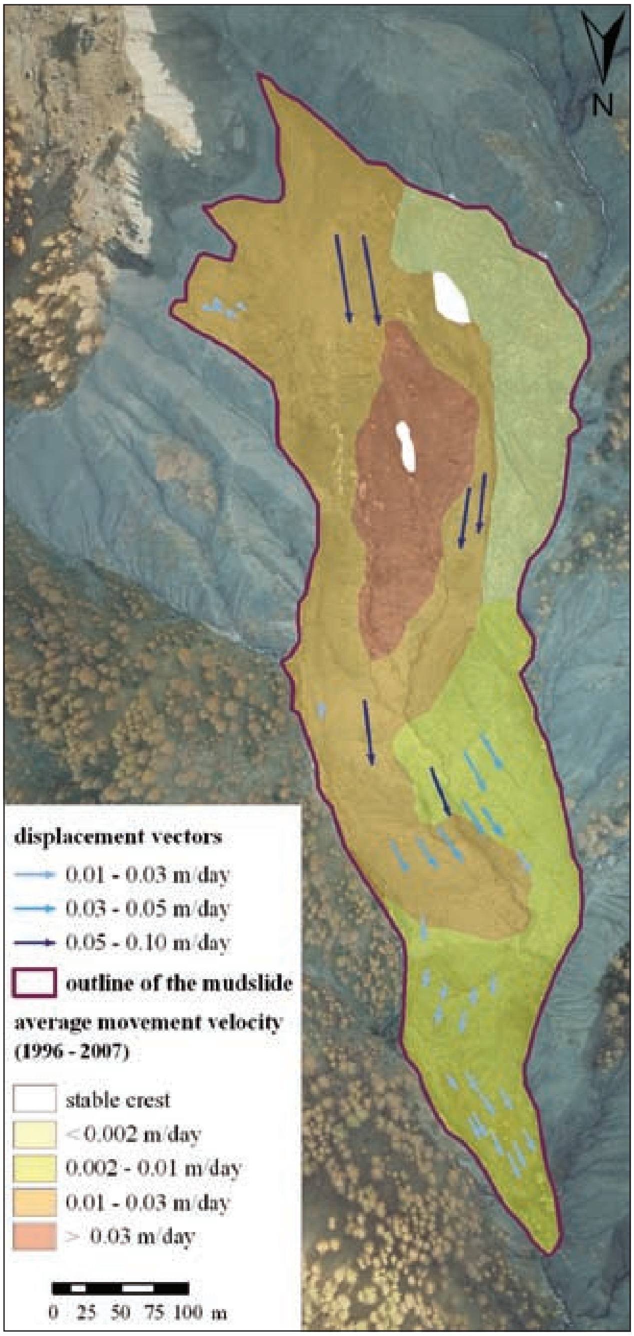

***Figure 6** Displacement vectors (blue colours) between May 2007 – October 2008 plotted on top of the average movement velocity map (1996-2007).*

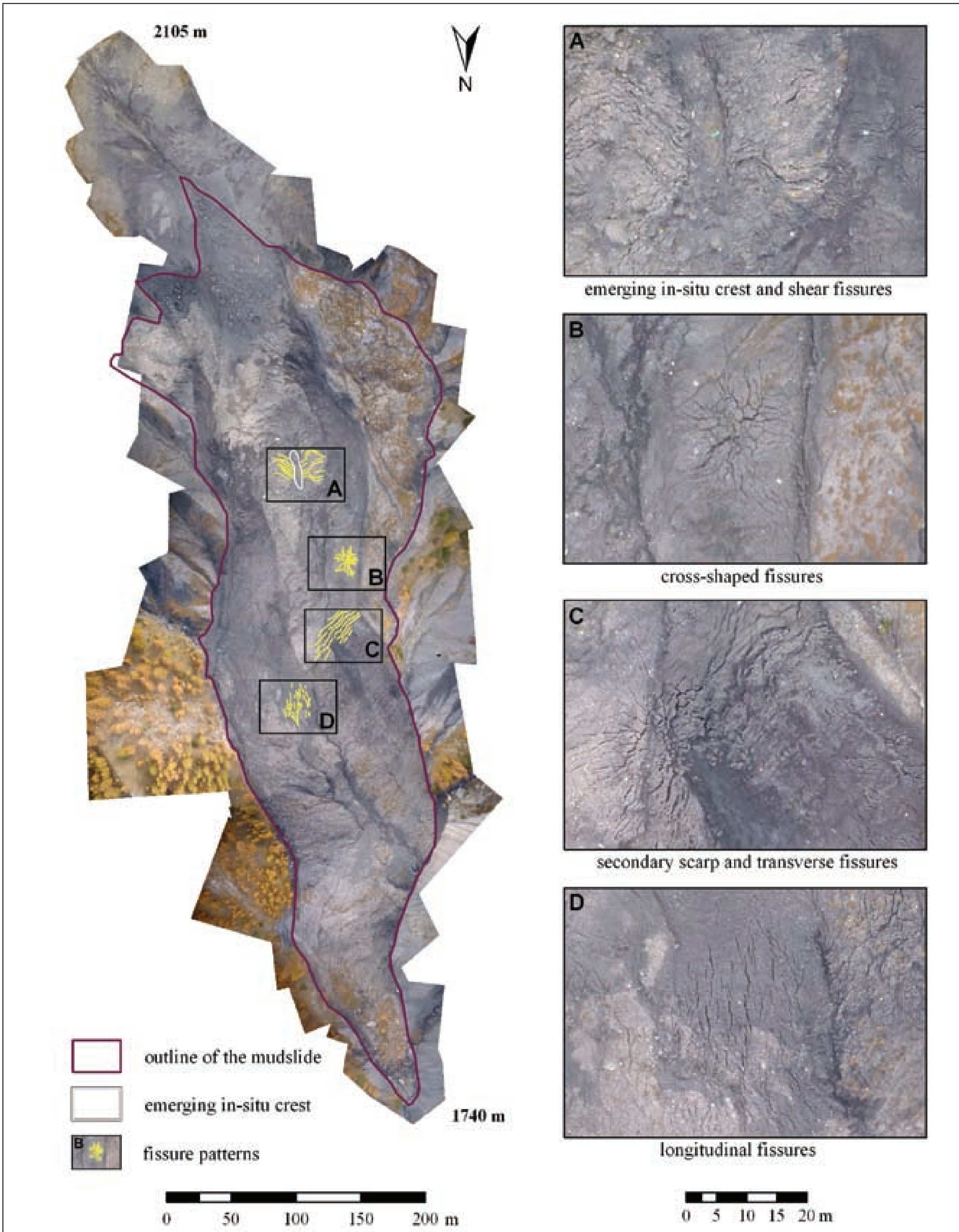

Figure 7 *Ortho-mosaic from pictures taken in October 2008 with locations of observed fissure patterns.*

cannot precisely determine the depth of the seismically observed events. They could occur within the mudslide, or along the mudslide bedrock interface. Remote sensing maps fissures but does not directly relate to the time history of generating processes. By chance, one of our seismometers dropped into a newly opened fissure on 22 July 2008. In the few hours before, we had observed four 'fracture' events close by, indicating recent fissure development. We therefore assume that 'fracture' signals are typically generated by fissure development in the shallow subsurface. This assumption is supported by observations of UAV-based remote sensing where fissure patterns could be observed for all cases where subsurface fracture propagated to surface rupture. Only in the uppermost section, the continuous drop of new material fills fissures shortly after opening. The process

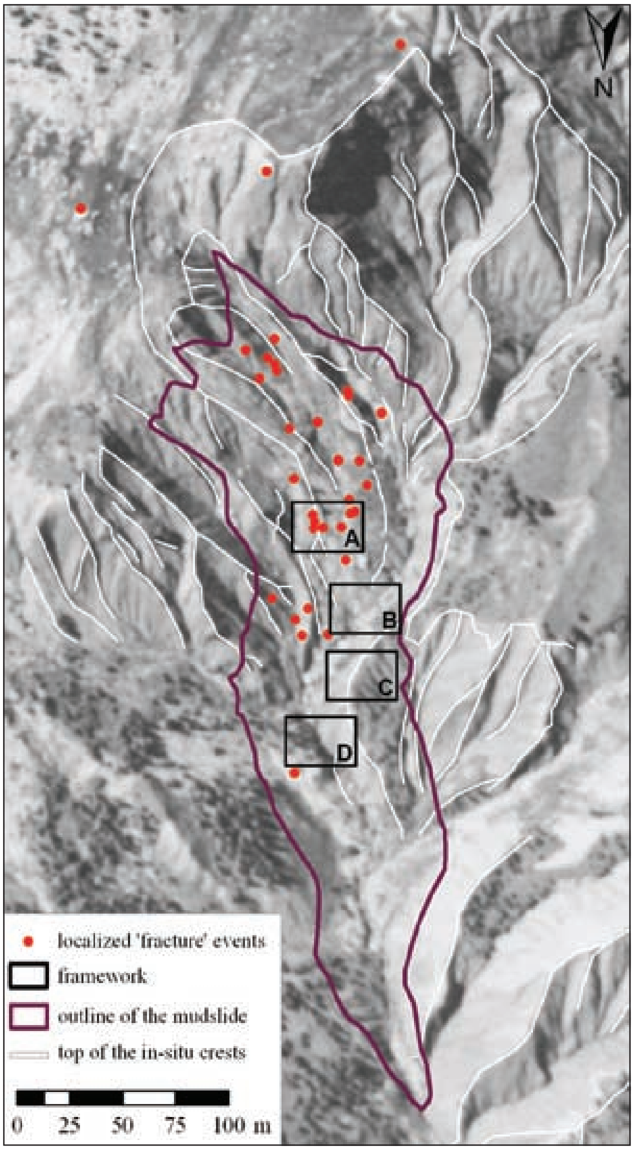

Figure 8 Epicentres of the localized 'fractures', determined displacement vectors (May 2007 – October 2008) and locations of remarkable fissure patterns (see figure 7) mapped on an airborne picture from 1956.

of rockfalls can be observed by 'rockfall' or impact signals in nanoseismic monitoring (Walter and Joswig, 2009).

More support of our hypothesis on source processes comes from field and lab observations. Below a depth of some one metre, the mudslide material is permanently water-saturated, but above, water saturation varies seasonally (Malet, 2003). For our observations of impulsive stress relief and fissure patterns, the material must deform in a brittle manner. The mudslide material shows highest shear strength in a range of 15–18 % water saturation (Malet, 2003). Once the snow melting period took place, the surface material dries out in summer, and the necessary material properties can be observed.

Our observations at the Super-Sauze mudslide also support prior investigations suggesting that the topography of the bedrock below the mudslide material plays a key role regarding the dynamic of the entire slope instability. By nanoseismic monitoring, we could observe numerous 'scratch' sequences that are generated within the shallow subsurface. Their energetic signature in the frequency-time domain is completely different to the impulsive 'fracture' signals. The vast majority of 'scratch' is bound to in-situ crests indicating scratching and grinding of single rock particles within the mudslide along the crests. Most sequences occur at emerging crests close to or above surface where rock particles are embedded in a shear resistant matrix of dried mud. Our hypothesis is supported by UAV-based remote sensing where several cross-shaped and shear fissures indicating dynamics according to in-situ crests are co-located to 'scratch' sites.

Conclusions

Applying the nanoseismic monitoring method we observed different seismic signals caused by the varying slope dynamics. Our preliminary hypothesis is that the 'fracture' events are caused by impulsive fracture processes within the unstable material. Similar signals have been observed at Heumoes slope consisting of weak sediments as well (Figure 2, Walter and Joswig, 2008). By contrast, we assume that the 'scratch' sequences are caused by 'scratching' and 'grinding' of single rocks in the slope material against the (emerging) in-situ crests (Walter and Joswig, 2009). Both processes are constrained by the uppermost metre where mudslide material dries out in summer to consolidate with sufficient shear resistance. Our ideas are supported by the existence of fissure patterns at the surface which could be observed by UAV-based remote sensing.

The joint observations by nanoseismic monitoring and UAV-based remote sensing in 2008 indicate that the varying tempo-spatial dynamics of the mudslide in Super-Sauze match the long-term observations. These dynamics are controlled by the fixed topography of the bedrock and the lateral hard rock boundaries where gullies between the crests 'canalize' the sliding material (Malet, 2003). Different fissure patterns at the surface are linked to abrupt changes of in-situ crest orientation in the shallow subsurface (Figure 8). Fissure patterns could be identified by comparison to glaciers where similar dynamics take place.

The joint observations of the mudslide in Super-Sauze indicate that the variations of tempo-spatial dynamics in 2008 are similar to the dynamics within the recent years. We can support prior observations (Malet, 2003) that the stable, buried in-situ crests at the bedrock of the mudslide directly affect the behaviour of the entire mudslide, and that gullies between the crests 'canalize' the sliding material. Several fissure patterns at the surface are linked to an abrupt change of the in-situ crests' orientation in the shallow subsurface (Figure 8).

Acknowledgements

We thank all colleagues from the OMIV project (Observatoire des Instabilités de Versants) for the helpful discussions and their support in the field. The authors are especially grateful to Jean-Philippe Malet (School and Observatory of Earth Sciences, University of Strasbourg) for providing several airborne pictures (Figures 4, 6, and 8) and datasets. Many thanks to Eberhard Claar (Institute for Geophysics, Universität Stuttgart) who built significant components of the quad-rotor system. The work is funded by the DFG within the project FOR 581 'Natural Slopes'.

References

Amitrano, D., Gaffet, S., Malet, J.-P. and Maquaire, O. [2007] Understanding mudslides through micro-seismic monitoring: the Super-Sauze (South-East French Alps) case study. *Bulletin de la Société Géologique de France* **178**(2), 149-157.

Brückl, E. and Mertl, S. [2006] Seismic Monitoring of Deep-Seated Mass Movements. *INTERPRAEVENT International Symposium 'Disaster Mitigation of Debris Flows, Slope Failures and Landslides.'* Universal Academy Press, Tokyo, Japan, 571-580.

de Montety, V., Marc, V., Emblanch, C., Malet, J.-P., Bertrand, C., Maquaire, O. and Bogaard, T.A. [2007] Identifying the origin of groundwater and flow processes in complex landslides affecting black marls: Insights from a hydrochemical survey. *Earth Surface Processes and Landforms*, **32**(1), 32-48.

Flageollet, J.-C., Malet, J.-P., Maquaire, O. and Schmutz, M. [2004] Integrated investigations on landslides: example of the Super-Sauze earthflow. In: Casale, R., Margottini, C. (Eds) *Natural Disasters and Sustainable Development*, Springer-Verlag, Berlin, 213-238.

Flageollet, J.-C., Malet, J.-P. and Maquaire, O. [1999] The 3D structure of the Super-Sauze earthflow: a first stage towards modelling its behaviour. *Physics and Chemistry of the Earth*, **25**(9), 785–791.

Flageollet, J.-C., Maquaire, O., Martin, B. and Weber, D. [1999] Landslides and climatic conditions in the Barcelonnette and Vars basins (Southern French Alps, France). *Geomorphology*, **30**, 65-78.

Grandjean, G., Malet, J.-P., Bitri, A. and Méric, O. [2007] Geophysical data fusion by fuzzy logic for imaging the mechanical behaviour of mudslides. *Bulletin de la Societe Geologique de France*, **178**(2), 127-136.

Hambrey, M. and Alean, J. [1994] *Glaciers*. Cambridge University Press, 208pp.

Hambrey, M. J. and Lawson, W. J. [2000] Structural styles and deformation fields in glaciers: a review. In: Maltman, A. J., Hubbard, B. and Hambrey, M. J. (Eds) Deformation of Glacial Materials, *Geol. Soc. Spec. Publ.*, **176**, 59–83.

Henry, J.-B, Malet, J.-P., Maquaire, O. and Grussenmeyer, P. [2002] The use of small-format and low-altitude aerial photos for the realization of high-resolution DEMs in mountainous areas: application to the Super-Sauze earthflow (Alpes-de-Haute-Provence, France) *Earth Surface Processes and Landforms*, **27**(12), 1339-1350.

Joswig, M. [2008] Nanoseismic Monitoring fills the gap between microseismic networks and passive seismic, *First Break*, **26**(6) 121-128.

Malet, J.-P. and Maquaire, O. [2003] Black marl earthflows mobility and long-term seasonal dynamic in southeastern France. In: Picarelli, L. (Ed) *International Conference on Fast Slope Movements: Prediction and Prevention for Risk Mitigation*, Patron Editore, Bologna, 333–340.

Malet, J.-P. [2003] *Les glissements de type écoulement dans les marnes noires des Alpes du Sud. Morphologie, fonctionnement et modélisation hydro-mécanique*. Thèse de Doctorat, Université Louis Pasteur, Strasbourg, 364pp.

Malet, J.-P., Maquaire, O. and Calais, E. [2002] The use of Global Positioning System for the continuous monitoring of landslides. Application to the Super-Sauze earthflow (Alpes-de-Haute-Provence, France). *Geomorphology*, **43**, 33-54.

Mikrocopter 2008. http://www.mikrocopter.de.

Niethammer, U., Rothmund, S. and Joswig, M. 2009. UAV-based remote sensing of the slow-moving landslide Super-Sauze. In: Malet, J.-P., Remaître, A., Boogard, T. (Eds) *Proceedings of the International Conference on Landslide Processes: from geomorpholgic mapping to dynamic modelling*, Strasbourg, CERG Editions: 69-74.

Roth, M., Dietrich, M., Blikra, L.H. and Lecomte, I. [2005] Seismic monitoring of the unstable rock slope at Åknes, Norway. *NORSAR Report for the International Centre for Geohazards*.

Spillmann, T., Maurer, H., Green, A. G., Heincke, B., Willenberg, H. and Husen, S. [2007] Microseismic investigations of an unstable mountain slope in the Swiss Alps. *J. Geophys. Res.*, **112**, B07301.

UAVP [2008] http://www.uavp.ch.

Varnes, D.J. [1978] Slope movement types and processes. In: Schuster, R. L. and Krizek, R. J. (Eds) *Landslides—Analysis and Control*. Rep. Natl. Res. Counc. Transp. Res. Board, **176**, 11–33.

Walter, M. and Joswig, M. [2008] Seismic monitoring of fracture processes generated by a creeping landslide in the Vorarlberg Alps. *First Break*, **26**(6), 131-135.

Walter, M. and Joswig, M. [2009] Seismic characterization of slope dynamics caused by softrock-landslides: The Super-Sauze case study. In: Malet, J.-P., Remaître, A., Boogard, T. (Eds) *International Conference on Landslide Processes: from geomorphologic mapping to dynamic modelling*, Strasbourg, CERG Editions, 215-220.

Wilhelm, F. [1975] *Schnee- und Gletscherkunde*. Walter de Gruyter Press, 434pp.

Wust-Bloch, G. H. and Joswig, M. [2006] Pre-collapse identification of sinkholes in unconsolidated media at Dead Sea area by Nanoseismic Monitoring, *Geophys. J. Int.*, **167**, 1220–1232.